NUKLEONIKA 2013;58(3):365–370

ORIGINAL PAPER

A review of phase transitions in RbIn-molybdate

Maria B. Zapart,
Włodzimierz Zapart

Abstract. The paper gives a brief review of the results of EPR temperature studies of $RbIn(MoO_4)_2$ crystal. A sequence of several structural phase transitions has been found in this crystal in the temperature region 84–163 K. The transition at $T_1 = 163$ K leads to an incommensurate triply modulated state, whereas ferroelastic phases start below $T_2 = 143$ K. All the low temperature phases in the temperature region 84–143 K are examples of simultaneously ferroelastic and incommensurate ones. The transition observed at $T_5 = 84$ K seems to suppress the ferroelastic properties of the crystal.

Key words: electron magnetic resonance (EMR) • trigonal double molybdates • incommensurate phase • ferroelastics • phase transitions

Introduction

Trigonal double molybdates and tungstates (TDM/T) of alkali and trivalent metals of general formula $AB(XO_4)_2$ (A = alkali metal, B = trivalent element, X = Mo, W) have attracted much attention in recent years because of their simple structure and the ability to undergo ferroelastic phase transitions in wide temperature ranges.

TDM/T are isostructural compounds with common crystal-chemical features [15] and the crystal structure of their high-temperature trigonal phases is described by the space group $P\bar{3}m1$ with one formula per unit cell. This structure is built up from the corner sharing BO_6 octahedra connected to the XO_4 tetrahedra. The A^+ ions are situated between these layers. The BO_6 octahedra centred on the B^{3+} have a trigonal symmetry.

Most of TDM/T undergo ferroelastic phase transitions of a displacive type. A group theoretical analysis of possible transitions in these compounds has shown that they lead to either monoclinic ($C2/m$ or $C2/c$) or triclinic ($P\bar{1}$) systems and are induced by one of the two-dimensional irreducible representations of the space group $P\bar{3}m1$, τ_5 or τ_6 [19]. The transition from the trigonal phase is improper and is accompanied by a doubling of the unit cell along the threefold axis of the crystal. In the TDM/T compounds the symmetry reduction from the trigonal to monoclinic phase leads to the occurrence of three orientational states S_i ($i = 1, 2, 3$) that are separated by two different types of domain walls called W and W' [13, 18].

M. B. Zapart✉, W. Zapart
Faculty of Materials Processing Technology
and Applied Physics,
Institute of Physics,
Technical University of Częstochowa,
19 Armii Krajowej Ave., 42-200 Częstochowa, Poland,
Tel.: +48 34 325 0619, Fax: +48 34 325 0795,
E-mail: zapart@wip.pcz.pl

Received: 17 August 2012
Accepted: 8 September 2012

EPR has proved to be a very useful technique for the investigation of ferroelastic phase transitions in these compounds [37, 39, 40]. EPR spectra of admixture ions have confirmed the reduction of point symmetry and the doubling of the unit cell along the c-axis in the low temperature phases. Also, on the basis of EPR studies models for the deformation of the high-temperature (HT) phase leading to the monoclinic systems *C*2/*c* or *C*2/*m* were proposed. It has been shown that EPR of Cr^{3+} ions may be used for evidencing the occurrence of ferroelastic domain structure [32].

In spite of the fact that the crystals have attracted the attention of researchers for a number of years, there still seem to be a lot of doubts regarding their properties. Recently, it has been pointed out that the ferroelastic phases realized in TDM/T may be simultaneously incommensurate [16, 30, 33, 35]. Thus, these crystals are regarded as examples of systems described by the multi-component order parameter. In this paper peculiarities connected with the phase transitions occurring in TDM/T are reviewed using as an example one member of this crystal family $RbIn(MoO_4)_2$.

Multi-q incommensurate states

The occurrence of a transition from a normal phase to a new phase presenting a structure with an incommensurate modulation has been observed in many different materials [7, 9]. For the incommensurate phases, the free energy is a minimum for the wave vector q_0 which is not a high-symmetry point of the Brillouin zone of the HT (normal) phase. Often the free-energy minima lie at several equivalent points related by symmetry operations of the high-temperature phase (the star of q_0). The modulated structure can then correspond to a set of domains with a single-wave (1 q) modulation corresponding to each pair ($\pm q_0$) of the star, or to a multi-q structure corresponding to the superposition of several waves with non-collinear wave vectors [12]. Phase transitions leading to such incommensurate phases are described by order parameters with a minimum dimensionality 2, 4 or 6 resulting in single-q, double-q or triple-q modulated structures [6, 8].

The shape of the resonance line in the incommensurate phase depends on the dimensionality of the modulation. Nuclear magnetic resonance (NMR), electron paramagnetic resonance (EPR) and nuclear quadrupole resonance (NQR) spectra and relaxation of incommensurate systems with a two-component order parameter corresponding to a one-dimensional modulation wave are now well understood; in these cases the averaged structure of the incommensurate phase has the same space group as that of the normal phase. The best known examples are the crystals of A_2BX_4 family [7, 9].

On the other hand, very little is known about the multi-q incommensurate systems. In the double-q or triple-q modulated structures two different incommensurate states may exist. The first one corresponds to the 2-q or 3-q structures with a simultaneous freezing of all vectors $\pm q_j$; the averaged structure of such an incommensurate phase has the same space group as that of the normal phase. Another possible state corresponds to a domain structure; each domain is here modulated in a single direction (1-q state), but the direction of modulation wave varies from one domain to another. In this case the symmetries of normal and incommensurate phases can be different. The double-q modulated structures have been found to realize in biphenyl [21, 27, 28], in barium sodium niobate, $Ba_2NaNb_5O_{15}$ [5, 26] or in $Cs_3Bi_2I_9$ [3]. The examples of triply modulated systems are quartz, SiO_2 [1, 11, 23, 24] and proustite Ag_3AsS_3 [17, 22, 25].

In the multi-q systems, transitions between the two different incommensurate phases can be observed. For example, the 1-q $\rightarrow$ 2-q transitions have been observed in barium sodium niobate [14, 20] and transitions 1-q $\rightarrow$ 3-q in proustite [4]. The mechanism of the 1-q $\rightarrow$ 3-q phase transition characteristic of the hexagonal system is discussed in [10].

Phase transitions in $RbIn(MoO_4)_2$

EPR of admixture ions led to the detection of a second-order phase transition at $T_1 = 163$ K in $RbIn(MoO_4)_2$ [31]. The transition was observed through the broadening of EPR lines of Cr^{3+} and Fe^{3+} ions. Figure 1 shows

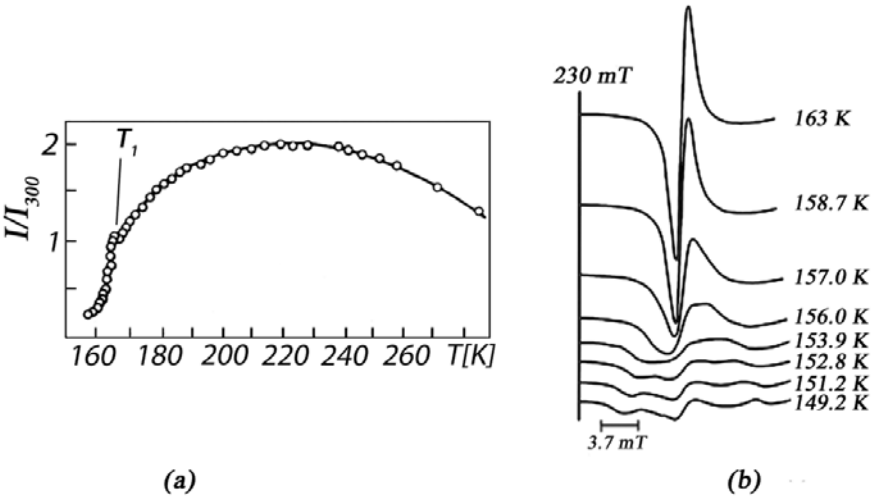

Fig. 1. Temperature changes in: (a) amplitude and (b) lineshape of the EPR line for Cr^{3+} in $RbIn(MoO_4)_2$ in the vicinity of first phase transition at $T_1 = 163$ K, for EPR line of the transition $|1/2> \leftrightarrow |-1/2>$.

the temperature behaviour of the EPR lines for Cr^{3+} ions in the stress free $RbIn(MoO_4)_2$ in the vicinity of T_1. Figure 1a shows temperature changes in the amplitude of the resonance line for transition $|1/2> \leftrightarrow |-1/2>$ whereas Fig. 1b presents the temperature changes of the EPR lineshape. Below 220 K, the intensity of the resonance line begins to decrease; it is accompanied with an increase of its linewidth. Below 163 K, the resonance line remains unresolved, but its amplitude rapidly decreases. One can notice that below 156 K the resonance line is spread into a broad continuum without any singularities.

According to the scheme of phase transitions in the TDM/T family given in [19] this transition should lead from the trigonal to monoclinic symmetry. Thus, the transformation to a ferroelastic phase should be seen through splitting of the EPR lines into a few components. The most striking effect is provided by no evidence of any changes in the crystal structure under the polarizing microscope in the temperature range 143–163 K [36], whereas a very pronounced evidence of such changes is found in EPR investigations.

The situation is well understood under the assumption that at $T_i = 163$ K a transition to an incommensurate 3-q state takes place in the crystal [29, 30]. The resonance field distribution in such a state is given by a multiple convolution [6] of field distributions $f(B_i)$ for purely one-dimensional modulations $B = B_0 + B_i \cos \varphi_i$

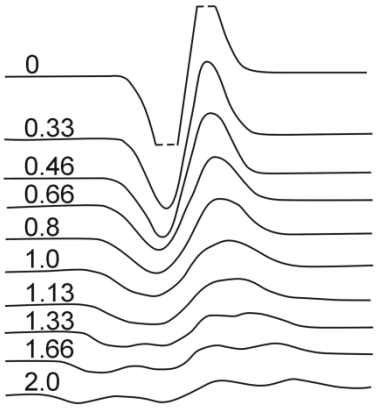

Fig. 2. Simulated EPR spectra for the 3-q state in the case of $B_1 = B_2$ and $B_3 \approx 0$, for various values of $B_1/\Delta B$.

$$f(B) = \int_{-\infty}^{\infty} f_1(B_1^{'}) f_2(B_2^{'}) \ldots f_{n-1}(B_{n-1}^{'}) \cdot f_n(B - \sum_{j=1}^{n-1} B_j^{'})\, dB_1^{'}\, dB_2^{'} \ldots dB_{n-1}^{'} \quad (1)$$

Accordingly to Eq. (1) in the 3-q state lineshape is given by a double convolution of the 1-q modulation distribution. The distribution functions have no singularities, but their derivatives have between four and six van Hove-type singular points depending on the ratios between B_i [6]. Making the use of such a distribution function we obtained simulated EPR spectra for the 3-q case as shown in Fig. 2. The simulated EPR spectra for the 3-q state are given for the case $B_1 = B_2 \neq 0$ and $B_3 = 0$. The spectra are obtained for different values of $B_1/\Delta B$, where ΔB is the EPR linewidth. The simulated lineshape reproduces characteristic features of the experimental line shape very well. The 3-q state model can describe the EPR lineshape in the temperature region 148–163 K [30].

The average crystal symmetry in this state should be the same as the one in the high temperature trigonal phase. This means that no change of the polarized light interaction within the crystal should take place on moving from the high temperature phase to the low temperature phase (3-q state) below 163 K. This statement is in agreement with the results of our polarized light microscopy studies of $RbIn(MoO_4)_2$ – no changes in the interference colours have been found in the crystal on cooling down to 143 K [36].

Very weak changes indicating the occurrence of the ferroelastic domain structure appear at around 143 K. The domain configuration observed in different thermal cycles was based on the W or W' walls. Lowering of the crystal symmetry in the vicinity of 143 K is also evidenced in the conoscopic images of $RbIn(MoO_4)_2$ [36]. The appearance of ferroelastic domain structure at 143 K coincides with another anomaly observed in the EPR spectra (Fig. 3a). One can see that close to 143 K the amplitude of all resonance lines reaches a maximum, the lines become narrow and well-separated. It has been suggested that at $T_2 = 143$ K a transition from the 3-q state to three-domain 1-q states appears [36]. The 1-q states are ferroelastic ones, which means

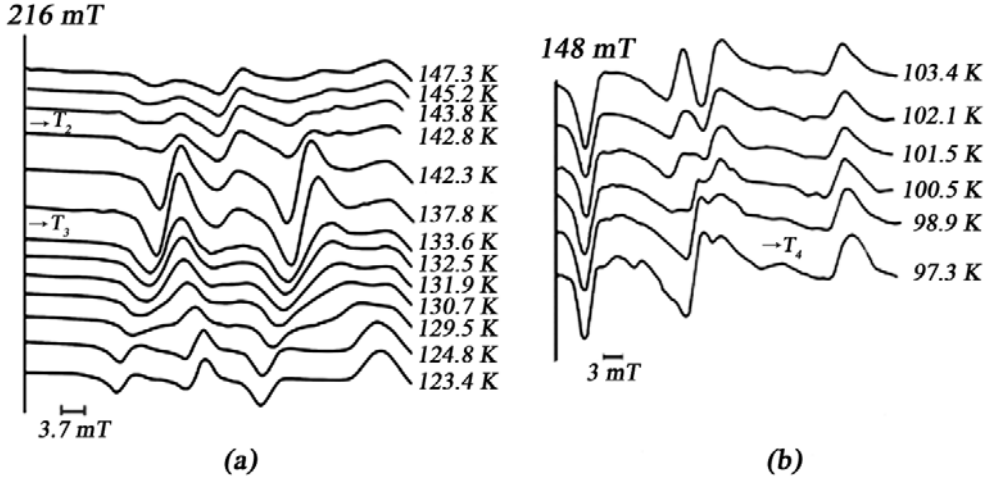

Fig. 3. Temperature changes of EPR spectra in $RbIn(MoO_4)_2$:Cr^{3+} for the transitions (a) $|1/2> \leftrightarrow |-1/2>$ and (b) $|-3/2> \leftrightarrow |-1/2>$.

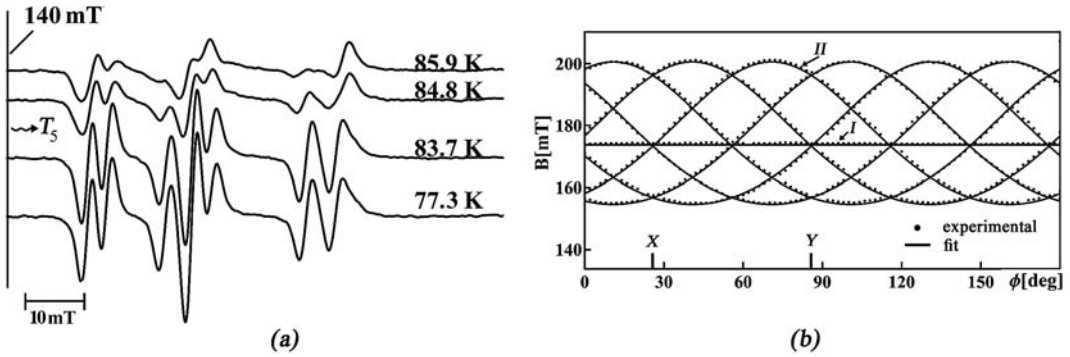

Fig. 4. (a) Temperature changes of the EPR spectra of $RbIn(MoO_4)_2$:Cr^{3+} in the vicinity of T_5 = 84 K for the transition $|-3/2> \leftrightarrow |-1/2>$ and magnetic field B lying in the XY plane; (b) Angular variation of the Cr^{3+} low-field lines in the XY plane at 77 K. The solid curves show the theoretical curves calculated using the spin Hamiltonian parameters from Table 1. The laboratory system of the X, Y and Z axes coincides with that of the crystallographic axes (X||2, Z||3).

that the average symmetry is lowered to the monoclinic one. The suggested space symmetry in this monoclinic phase is $C2/c$.

On further cooling, the crystal, the width of resonance lines starts to increase and their amplitude slowly drops. Anomalies in the EPR spectra of Cr^{3+} indicate that at T_3 = 134 K (Fig. 3a) and T_4 = 98 K (Fig. 3b) other phase transitions take place [34]. The temperature region around 98 K, in which anomalies in the EPR line behaviour occur in $RbIn(MoO_4)_2$, coincides with that in which rebuilding of the domain structure takes place in this crystal; the domains are very homogeneous with a preferential type of the W walls [36].

Below 98 K, seven broad and overlapping component resonance lines are observed (Fig. 4). The nature of transitions at T_3 and T_4 is still unclear. However, the presence of broadened EPR lines and the ferroelastic domains suggest that these transitions lead to simultaneously incommensurate and ferroelastic phases. In the temperature range from 85 to 97 K the resonance lines change only slightly with temperature. As seen in Fig. 4a, significant changes in the EPR spectrum start below 85 K and at around T_5 = 84 K, instead of broad overlapping lines, seven intense well-separated resonance lines are observed. Both the temperature behaviour of EPR lines as well as motion of the phase front observed under polarizing microscope indicate the phase transition at about T_5 being of the first order.

Surprisingly, it was found that below T_5 the ferroelastic phase disappears [38]. This phase transition was confirmed by dynamical mechanical analysis (DMA) through anomalies in the temperature behaviour of both real and imaginary parts of the Young's modulus [38].

From the anisotropy patterns, seven kinds of Cr^{3+} complexes are identified that can be divided into two structurally in-equivalent groups (marked as I and II in Fig. 4b). The chromium complexes of type I lie in the axial crystal field with the principal z-axis parallel to the threefold crystal Z-axis. The type II group consists of six magnetically in-equivalent kinds of paramagnetic centres lying in the crystal field of lower symmetry with their z-axes deviated from the Z-axis.

The EPR spectrum of the Cr^{3+} centre (S = 3/2) is described by spin Hamiltonian in the form [2]:

$$H = \mu_B B \cdot g \cdot S + \frac{1}{3}(b_2^0 O_2^0 + b_2^2 O_2^2) \qquad (2)$$

where μ_B is the Bohr magneton, O_n^m are the Stevens operators, b_n^m are the zero-field splitting (ZFS) parameters, g is the spectroscopic tensor. The values of the spin Hamiltonian parameters which characterize these two groups of Cr^{3+} complexes and the disposition of the principal axes of their D-tensors are collected in Table 1. For comparison, the parameters of spin Hamiltonian for Cr^{3+} complexes are listed in the HT phase

Table 1. Spin Hamiltonian parameters and direction cosines of Cr^{3+} centres in $RbIn(MoO_4)_2$ at temperatures 300 K (paraelastic phase), 142 K (ferroelastic phase) and 77 K (non-ferroelastic phase). The direction cosines are referred to the XYZ axis system

Temperature (K)		g	b_2^0 (cm^{-1})	b_2^2 (cm^{-1})	Direction cosines			Ref.
300		$g_{\|\|}$ = 1.964 $g_\perp$ = 1.968	0.540	0	– – 0	– – 0	0 0 1	[40]
142		g_x = 1.968 g_y = 1.968 g_z = 1.965	0.549	0.045	0.9659 –0.2588 0.0045	0.2588 0.9658 –0.0168	0 0.0174 0.9998	
77	I	$g_{\|\|}$ = 1.964 $g_\perp$ = 1.968	0.552	0	– – 0	– – 0	0 0 1	[38]
	II	g_x = 1.968 g_y = 1.968 g_z = 1.965	0.552	0.141	0.9659 –0.2580 0.0203	0.2588 0.9629 –0.0758	0 0.0758 0.9969	

as well as in the phase limited to the temperature range $T_2 < T < T_3$.

The simplest model of the unit cell deformation explaining the presence of Cr^{3+} complexes of type I and II below 84 K was given in [38]. The disposition of the principal axes of the *D*-tensors of Cr^{3+} complexes showing the Laue class $\bar{3}m$ as found from the anisotropy patterns taken at 77 K, and the lack of ferroelastic domain structure below 84 K indicate that, despite large changes in the crystal structure, the transition to the lowest phase restores the trigonal symmetry.

Final remarks

Upon lowering the temperature, a sequence of phase transitions was found in the $RbIn(MoO_4)_2$ crystal as evidenced by anomalies in the electron paramagnetic resonance spectra of paramagnetic admixture ions as well as through changes in the ferroelastic domain structure. The transition at 163 K takes the crystal from the trigonal to incommensurate 3-q phase, and then to a three-domain 1-q state at 143 K.

Subsequent transformations are found at 134 K and 98 K; the sequence ends with a transition at 84 K in which the trigonal symmetry seems to be restored. This low-temperature phase of $RbIn(MoO_4)_2$ seems to be new, unknown in the family of TDM/T crystals. A certain ferroic ordering like antiferroelasticity or ferrogyrotropy could be speculated to exist in this phase. However, to prove it additional experiments are required.

References

1. Abe K, Kawasaki K, Kowada K, Shigenari T (1991) Effect of uniaxial stress on central peaks in the 1q and 3q incommensurate phase of quartz. J Phys Soc Jpn 60:404–407
2. Abragam A, Bleaney B (1970) Electron paramagnetic resonance of transition ions. Clarendon Press, Oxford
3. Aleksandrova IP, Sukhovsky AA, Aleksandrov KS (1998) Novel incommensurate phase in $Cs_3Bi_2I_9$. Solid State Commun 105:323–326
4. Apih TU, Mikac TU, Seliger J, Dolinsek J, Blinc R (1998) Evidence for a 1-*q* to 3-*q* transition and 3-*q* soliton lattice in incommensurate proustite. Phys Rev Lett 80:2225–2228
5. Barre S, Mutka H, Roucau C *et al*. (1991) Influence of defects on the incommensurate modulation in irradiated $Na_2NaNb_5O_{15}$. Phys Rev B 43:11154–11161
6. Blinc R, Apih T (2002) NMR in multidimensionally modulated incommensurate and CDW systems. Prog Nucl Reson Spectrosc 41:49–82
7. Blinc R, Prelovsek P, Rutar V, Seliger J, Zumer S (1986) Experimental observations of incommensurate phases. In: Blinc R, Levanyuk AP (eds) Incommensurate phases in dielectrics. 1. Fundamentals. North-Holland Publishing, Amsterdam, pp 143–276
8. Blinc R, Zumer S (1990) NMR line shapes and relaxation in incommensurate systems with a multiple-q modulation. Phys Rev B 41:11314–11318
9. Cummins HZ (1990) Experimental studies of structurally incommensurate crystal phases. Phys Rep 185:211–411
10. Dmitriev SV, Shigenari T, Abe K (1998) Mechanism of transition between 1q and 3q incommensurate phases in two-dimensional crystal model. Ferroelectrics 217:179–187
11. Dolino G (1986) The incommensurate phase of quartz. In: Blinc R, Levanyuk AP (eds) Incommensurate phases in dielectrics. 2. Materials. North-Holland Publishing, Amsterdam, pp 205–232
12. Dolino G, Bastie P, Berge B *et al*. (1987) Stress-induced 3-*q*-1-*q* incommensurate phase transition in quartz. Europhys Lett 3:601–699
13. Dudnik EF, Stolpakova TM, Kiosse GA (1986) Prostranstvennaya simmetria i osobiennosti segnetoelasticheskikh fazovykh perekhodov v trigonalnykh dvojnykh molibdatakh i volframatakh. Izv Akad Nauk SSSR Seria Fizika 50:2249–2251
14. Kiat JM, Uesu Y, Akutsu M, Aubree J (1992) Direct optical observation of the 1q/2q transition in incommensurate $Ba_2NaNb_5O_{15}$. Ferroelectrics 125:227–232
15. Klevtsova RF, Klevtsov PV (1970) Synthesis and crystal structure of the double molybdates $KR(MoO_4)_2$ for R^{3+} = Al, Sc, and Fe, and of the tungstate $KSc(WO_4)_2$. Kristallografiya 15:953–959
16. Mączka M, Kojima S, Hanuza J (1998) Heat capacity measurements of the normal incommensurate and lock-in transitions in $KSc(WO_4)_2$ and $KSc(MoO_4)_2$. J Phys Chem Solids 59:1429–1432
17. Norcross JA, Ailion DC (1996) ^{109}Ag NMR lineshape study of the 3*q* incommensurate insulator proustite (Ag_3AsS_3). Solid State Commun 98:119–122
18. Otko AI, Krainyuk GG, Stolpakova TM, Nosenko AE (1984) Domain switching and crystallographic features of monoclinic ferroelastic phases of some double molybdates and tungstates. Izv Akad Nauk SSSR Seria Fizika 48:1116–1119
19. Otko AI, Nesterenko NM, Povstyanyi LV (1978) Phenomenological approach to structural phase transitions in trigonal double molybdates and tungstates. Phys Status Solidi A 46:577–587
20. Pan X, Unruh H-G, Feng D (1990) TEM study of the 1q to 2q transition within the incommensurate phase of barium sodium niobate. Ferroelectrics 105:225–230
21. Parlinski K, Schranz W, Kabelka H (1989) Phenomenological theory of incommensurate phases in biphenyl. Phys Rev B 39:488–494
22. Ryan TW, Gibaud A, Nelmes RJ (1985) An X-ray scattering study of the modulated phases in proustite. J Phys C 18:5279–5287
23. Saint-Gregoire P, Luk'yanchuk I (1997) Domain textures of multi-q modulated phases; example of quartz. Ferroelectrics 191:267–273
24. Saint-Gregoire P, Luk'yanchuk I, Snoeck E, Roucau C, Janovec V (1996) A novel type of incommensutate phase in quartz: the elongated-triangle phase. Pisma Zh Eksp Teor Fiz 64:376–381
25. Subramanian RK, Muntean L, Norcross JA, Ailion DC (2000) ^{109}Ag NMR investigation of atomic motion in the incommensurate and paraelectric phases of proustite (Ag_3AsS_3). Phys Rev B 61:996–1002
26. Toledano JC, Schneck J, Errandonea G (1986) Incommensurate phase of barium sodium niobate. In: Blinc R, Levanyuk AP (eds) Incommensurate phases in dielectrics. 2. Materials. North-Holland Publishing, Amsterdam, pp 233–251
27. von Laue L, Ermark F, Gölzhäuser A, Haeberlen U, Häcker U (1996) Structural modulation and low-frequency excitations in the incommensurate phases of biphenyl. J Phys: Condens Matter 8:3977–3992
28. Véron A, Emery C, Spiesser M (1994) Domain structure in biphenyl incommensurate phase II observed by electron paramagnetic resonance. J Phys I France 4:1705–1723
29. Zapart MB (1992) Possibility of multi-q state in incommensurate $RbIn(MoO_4)_2$. Ferroelectrics 137:199–203

30. Zapart MB (1993) Incommensurate ferroelastics by electron paramagnetic resonance. Ferroelectrics 141:67–72
31. Zapart MB, Stankowski J, Sczaniecki PB, Otko AI (1979) Anomaly of Fe^{3+} EPR spectrum in $RbIn(MoO_4)_2$ monocrystal in the phase transition neighbourhood. Acta Phys Pol A 56:445–447
32. Zapart W (1989) Electron paramagnetic resonance in investigations of ferroelastic domain structure. Ferroelectrics 97:137–145
33. Zapart W (1990) Possibility of simultaneously incommensurate and ferroelastic phase in $RbIn(MoO_4)_2$ by EPR of Cr^{3+} ion. Phys Status Solidi A 118:477–454
34. Zapart W (1990) The successive phase transitions in $RbIn(MoO_4)_2$ studied by EPR of admixture ions. Ferroelectrics 105:291–296
35. Zapart W, Zapart MB (1990) Incommensurate phase in $KSc(MoO_4)_2$ by EPR of Cr^{3+}. Phys Status Solidi A 121:K43–K45
36. Zapart W, Zapart MB (2011) Effect of ferroelastic domain pattern changes on the EPR spectra in TDM. Phase Transitions 84:872–884
37. Zapart W, Zapart MB, Reng P, Hanuza J, Mączka M (2006) Ferroelastic phase transition in $KSc(WO_4)_2$: EPR of Gd^{3+}. Ferroelectrics 337:117–129
38. Zapart W, Zapart MB, Schranz W, Reinecker M (2013) Low temperature phase of the trigonal $RbIn(MoO_4)_2$ crystal. Phase Transitions 86:123–130
39. Zapart MB, Zapart W, Stankowski J, Zviagin AI (1982) Ferroelastic phase transitions in $KSc(MoO_4)_2$ monocrystals by electron paramagnetic resonance of Cr^{3+} ions. Physica B & C 114 B:201–211
40. Zapart MB, Zapart W, Zviagin AI (1984) Phase transitions in ferroelastic $RbIn(MoO_4)_2$ crystals by electron paramagnetic resonance of Cr^{3+} ions. Phys Status Solidi A 82:67–73